Available online at www.sciencedirect.com
ScienceDirect
Journal of Sound and Vibration 313 (2008) 418–432
JOURNAL OF SOUND AND VIBRATION
www.elsevier.com/locate/jsvi

Active scattering control of flexural waves at beam junctions: The influence of beam properties on power flow and control effort

Jonas L. Svensson[a,*], Patrik B.U. Andersson[a], Joachim Scheuren[b,1], Wolfgang Kropp[a]

[a]*Division of Applied Acoustics, Chalmers University of Technology, 41296 Göteborg, Sweden*
[b]*Müller-BBM GmbH, 82152 Planegg, Germany*

Received 26 July 2007; received in revised form 12 December 2007; accepted 12 December 2007
Handling Editor: C. Morfey
Available online 22 January 2008

Abstract

As a wave, propagating in a beam, enters a discontinuity it will be partly reflected and partly transmitted. The introduction of an external force can be used to impose restrictions on the scattering properties of the discontinuity. This phenomenon has been studied in the past, usually with the objective of changing the scattering properties of a free end. The purpose of this study is to investigate the effect of material parameters and cross-sectional dimensions on the control effort and power flow through a beam discontinuity, given a certain control objective. Active scattering factors, based on Euler–Bernoulli theory, are derived for the junction of two beams, with rectangular cross-sections. Desired constraints are put on one or several of these scattering factors and the equivalent required force is calculated. The control objectives studied are: a non-reflective junction, a non-transmissive junction and the minimisation of power flowing from the junction back into the beams. Derived expressions show that the control forces can, after normalisation, be expressed in a two-dimensional space (plane) for all possible material parameter and cross-sectional dimension combinations. In their limits these planes also contain the ideal termination cases. Thus, e.g. the required control forces in order to achieve a non-reflective junction for a clamped or free beam end are covered by these results. The transmission and reflection efficiencies for the different control objectives can also be depicted in the same plane. Results indicate the possibility of choosing a right-side beam and active force combination in such a way that the junction is anechoic and absorptive.

1. Introduction

The field of noise and vibration abatement occupies several engineers and researchers today. Vibration treatments can be studied from many points of view. The application decides the objective of the control. Traditionally vibration control can be divided into two main groups, passive or active treatments.

*Corresponding author. Tel.: +46 31 772 2209; fax: +46 31 772 2212.
E-mail address: jonas.svensson@chalmers.se (J.L. Svensson).
[1]This work was carried out under the author's adjunct professorship at the division of Applied Acoustics at Chalmers University of Technology.

0022-460X/$ - see front matter © 2008 Elsevier Ltd. All rights reserved.
doi:10.1016/j.jsv.2007.12.011

During the last 20 years there have been several publications devoted to different aspects of active vibration control. Because of their frequent appearance in structures, slender beams have been the topic of many of these research papers. Quite a few of these papers involve control of different wave modes in slender beams or at junctions between such beams. It is obvious that the geometry and material parameters of the involved beams play an important role for control effort and power flow through such a junction.

The purpose of this study is to investigate the influence of geometry and material parameters on control effort and power flow, given a certain control law. Two semi-infinite beams are connected and an active force is introduced in the junction. Three different control laws are derived and the power flow through this junction as well as the control effort are investigated while varying the difference in material parameters and cross-sectional dimensions between the two beams.

Structural networks, which frequently occur in several industrial applications, can contain junctions between slender beams of quite different properties. There may be changes in cross-sectional dimensions, density or stiffness. The so-called impedance mismatch between the beams will cause the incident power to be partly transmitted and partly reflected. This phenomenon has been studied in several publications.

The passive junction properties between two coupled beams have been published in *Structure Borne Sound* by Cremer et al. [1]. An incident wave is considered and the scattering properties of the junction are described by two transmission and two reflection factors, describing the propagating wave and near field, respectively. The derivation is based on Euler–Bernoulli beam theory.

In 1984 Mace [2] presented a paper where full transmission and reflection matrices were derived for both incident wave and near field simultaneously. Thus the scattering properties were described in 2×2 matrices. These derivations were also based on Euler–Bernoulli beam theory.

In 2005 Mei and Mace [3] presented a paper where the transmission and reflection matrices are derived for Timoshenko beam theory. Again the scattering properties (amongst many other results) are presented as two 2×2 matrices connecting propagating deflection and rotation waves at a junction between two semi-infinite beams.

For some cases it might be desirable to have a junction which reflects/transmits a certain portion of the incident power. It is easy to imagine a situation where an anechoic junction, which is obtained by avoiding any reflection of power, is advantageous. Therefore, attention has been focused on using active control as a part of the junction between one-dimensional waveguides, such as beams.

Miller [4] described the possibility of using active control at the junction point of one or several slender beams. Several control laws satisfying different control criteria were derived. Also several simple examples were given where the theory was applied to different structures, such as rods and beams. The control laws considered included forcing certain scattering properties upon the junction or absorbing power by optimal controllers. The theory has also been applied to more complex structures like the modelling of a satellite. Similar studies were presented by Miller and von Flotow [5], Miller et al. [6,7], and by von Flotow and Schäfer [8].

Several other authors have also studied active modification of scattering properties in beams. The control law that seems to have been studied the most in this case is the one that cancels reflection from a junction, normally that of a free end. Scheuren [9], Guardia and Bustamente [10], and Hu and Lin [11] all investigated, theoretically or experimentally, how to achieve a non-reflective/anechoic termination on a free end.

Other authors have studied active control configurations where the control objective has been selective wave cancellation. McKinnel [12] investigated the possibility to isolate a region of a waveguide by active cancellation of flexural waves. Mace [13] used secondary forces to actively clamp a flexural waveguide (beam) at a point, thereby hindering transmission beyond that point. Scheuren [14] dealt with suppression of selective wave mode amplitudes. Multipoint measurements enabled the separation of wave modes. The purpose of that study was to investigate the possibility of actively reflecting a propagating wave.

Focus has also been on various types of controllers to absorb energy with different approaches. Guicking et al. [15] used a tapered transmission line model and an impedance approach to actively absorb wave mode power. The beam impedance was matched to the impedance of an active load in order to maximise the power absorption. A paper by Brennan et al. [16] was published in 1995 investigating three fundamental control objectives: wave suppression, maximisation of actively absorbed power, and minimisation of the total input power introduced by both the primary and the secondary disturbance.

The study presented here investigates how the impedance mismatch between two beams connected through an active junction influences the power flow, given a certain control objective. The investigated control laws are: cancellation of reflected or transmitted wave, and the minimisation of scattered power. The power flow through this junction as well as the control effort are studied for different material parameter combinations of the two beams. The study is limited to non-dissipative, Euler–Bernoulli beams with rectangular cross-sections.

2. Euler–Bernoulli beam model

If the flexural wavelength is large in comparison to the cross-sectional dimensions of a beam, the Euler–Bernoulli theory gives a relatively accurate description of the deflection field on the beam. The Euler–Bernoulli bending wave equation is based on the fact that for low-frequency vibrations the bending motion is dominant. The Euler–Bernoulli theory neglects rotational inertia and shear deformation (i.e. infinite shear stiffness). The homogeneous partial differential equation is

$$EI\frac{\partial^4}{\partial x^4}w+\rho S\frac{\partial^2}{\partial t^2}w=0, \tag{1}$$

where w represents deflection, ρS is mass (per unit length) and EI is the bending stiffness. If the system experiences harmonic motion it can be assumed that a solution to the differential equation has the form of a wave:

$$\tilde{w}(x,t)=\hat{w}\mathrm{e}^{kx}\mathrm{e}^{\mathrm{j}\omega t}, \tag{2}$$

where k is the wavenumber, ω is the angular frequency, x is the length coordinate of the beam, t is the time, j is the imaginary unit and $\hat{w}$ is the amplitude of the wave. Inserting the expression for $\tilde{w}$ (Eq. (2)) into the differential equation (Eq. (1)) yields the dispersion relation,

$$k^4=\frac{\rho S}{EI}\omega^2. \tag{3}$$

From this four complex roots are acquired:

$$k_{\mathrm{I}}=-\mathrm{j}k_B,\quad k_{\mathrm{II}}=\mathrm{j}k_B,\quad k_{\mathrm{III}}=-k_B,\quad k_{\mathrm{IV}}=k_B, \tag{4a,b,c,d}$$

where k_B represents the bending wavenumber, given by

$$k_B=\sqrt{\omega}\sqrt[4]{\frac{\rho S}{EI}}. \tag{5}$$

The roots in Eqs. (4a,b,c,d) are inserted into the wave solution (Eq. (2)), which yields four different wave components, two propagating waves and two exponentially decaying components, the latter being so-called evanescent waves or near fields. The normal displacement field of the beam is the sum of these waves and near fields with the amplitudes adjusted according to the external excitation and boundary conditions.

A semi-infinite beam has only one boundary; thus a wave that is propagating away from this boundary will never be reflected, as seen on the right-side beam in Fig. 1. If a finite beam on the left side is connected to a semi-infinite beam on the right side and the excitation is located somewhere in the left-side beam (referring to

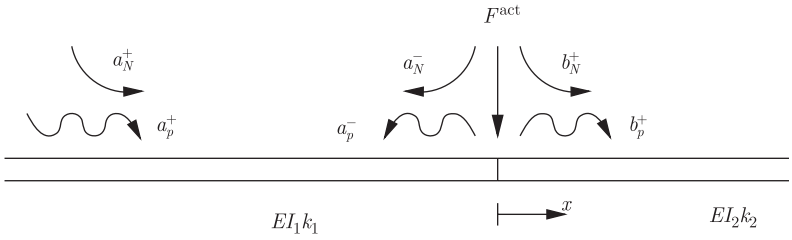

Fig. 1. The waves present on a finite beam connected to a semi-infinite beam with different properties. The primary excitation is assumed to be somewhere in the left-side beam and an active force is located at the junction.

Fig. 1), the deflection fields of the beams can be expressed as

$$w_1 = a_p^+ e^{-jk_1 x} + a_N^+ e^{-k_1 x} + a_p^- e^{jk_1 x} + a_N^- e^{k_1 x}, \quad w_2 = b_p^+ e^{-jk_2 x} + b_N^+ e^{-k_2 x}, \tag{6a,b}$$

where k_1 and k_2 represent the bending wavenumbers for the left- and right-side beams, respectively, and where the time dependence has been suppressed. The amplitudes are expressed with a for the left-side beam and with b for the right-side beam. They are subscribed with p or N for propagating wave or near field, respectively. The superscripts + or − indicate the propagation direction being the positive or negative x-direction (see Fig. 1). It is convenient to express the wave amplitudes in vector form as

$$\mathbf{a}^+ = \begin{Bmatrix} a_p^+ \\ a_N^+ \end{Bmatrix}, \quad \mathbf{a}^- = \begin{Bmatrix} a_p^- \\ a_N^- \end{Bmatrix}, \quad \mathbf{b}^+ = \begin{Bmatrix} b_p^+ \\ b_N^+ \end{Bmatrix}. \tag{7a,b,c}$$

These wave amplitudes can be related by introducing a reflection (**r**) and a transmission (**t**) matrix:

$$\mathbf{b}^+ = \mathbf{t}\mathbf{a}^+, \quad \mathbf{a}^- = \mathbf{r}\mathbf{a}^+. \tag{8a,b}$$

The exponential functions in Eqs. (6a,b) can be expressed in propagation matrices:

$$\mathbf{\Psi}_{\mathbf{a}^+} = \begin{bmatrix} e^{-jk_1 x} & 0 \\ 0 & e^{-k_1 x} \end{bmatrix}, \quad \mathbf{\Psi}_{\mathbf{a}^-} = \begin{bmatrix} e^{jk_1 x} & 0 \\ 0 & e^{k_1 x} \end{bmatrix}, \quad \mathbf{\Psi}_{\mathbf{b}^+} = \begin{bmatrix} e^{-jk_2 x} & 0 \\ 0 & e^{-k_2 x} \end{bmatrix}. \tag{9a,b,c}$$

For the beam element described in Fig. 2, the deflection (w), rotation (β), moment (M) and force (F) are related through

$$\beta = \frac{\partial w}{\partial x}, \quad M = -EI\frac{\partial \beta}{\partial x}, \quad F = -\frac{\partial M}{\partial x}. \tag{10a,b,c}$$

Using these relations, continuity of deflection and slope can, at any point, be stated according to

$$\begin{bmatrix} 1 & 1 \\ -j & -1 \end{bmatrix} \mathbf{\Psi}_{\mathbf{a}^+} \mathbf{a}^+ + \begin{bmatrix} 1 & 1 \\ j & 1 \end{bmatrix} \mathbf{\Psi}_{\mathbf{a}^-} \mathbf{a}^- = \begin{bmatrix} 1 & 1 \\ -j\gamma & -\gamma \end{bmatrix} \mathbf{\Psi}_{\mathbf{b}^+} \mathbf{b}^+ \tag{11a}$$

and equilibrium of moments and forces according to

$$\begin{bmatrix} 1 & -1 \\ j & -1 \end{bmatrix} \mathbf{\Psi}_{\mathbf{a}^+} \mathbf{a}^+ + \begin{bmatrix} 1 & -1 \\ -j & 1 \end{bmatrix} \mathbf{\Psi}_{\mathbf{a}^-} \mathbf{a}^- = \alpha \begin{bmatrix} 1 & -1 \\ j\gamma & -\gamma \end{bmatrix} \mathbf{\Psi}_{\mathbf{b}^+} \mathbf{b}^+, \tag{11b}$$

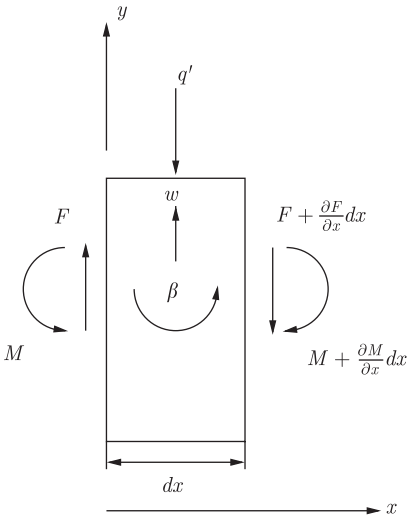

Fig. 2. Definition of the positive direction for the field variables. w indicates lateral displacement, β slope, M moment and F force.

where the substitutions α and γ have been introduced. They are defined as

$$\alpha = \frac{EI_2 k_2^2}{EI_1 k_1^2}, \quad \gamma = \frac{k_2}{k_1}. \tag{12a,b}$$

Substituting Eqs. (8a,b) into Eqs. (11a) and (11b), the transmission and reflection matrices (**r** and **t**) can be calculated to give

$$\mathbf{t} = \frac{2}{\Delta}\begin{bmatrix} (1+\gamma)(\alpha-1) & (1-\mathrm{j}\gamma)(1-\alpha) \\ (1+\mathrm{j}\gamma)(\alpha-1) & (1+\gamma)(1+\alpha) \end{bmatrix} \tag{13a}$$

and

$$\mathbf{r} = \frac{1}{\Delta}\begin{bmatrix} 2\alpha(1-\gamma^2) - \mathrm{j}\gamma(1-\alpha)^2 & \gamma(1+\mathrm{j})(1-\alpha^2) \\ \gamma(1-\mathrm{j})(1-\alpha^2) & 2\alpha(1-\gamma^2) + \mathrm{j}\gamma(1-\alpha)^2 \end{bmatrix}, \tag{13b}$$

where

$$\Delta = 2\alpha(1+\gamma^2) + \gamma(1+\alpha)^2. \tag{14}$$

For simplicity the connection point has been chosen at $x = 0$ as this reduces the propagation matrices to identity matrices. The matrices **t** and **r** are virtually the same 2×2 matrices as derived in Ref. [2], except for a slightly different notation.

3. Active beam junction

3.1. Active scattering properties

If the excitation in the left-side beam is considered to be far away in relation to the wavelength, the incoming near field can be neglected and the element related to the near field in the propagation matrix (element 2,2) in Eq. (9a) is replaced by a zero. If a gain matrix **G** is defined as

$$\mathbf{G} = \frac{1}{k_1^3 EI_1 a_p^+}\begin{bmatrix} 0 & 0 \\ F^{\mathrm{act}} & 0 \end{bmatrix}, \tag{15}$$

where F^{act} is an external force, then an actuation vector can be calculated as

$$\mathbf{Q}^{\mathrm{act}} = \mathbf{G}\mathbf{a}^+. \tag{16}$$

The actuation vector may also contain a moment term which would allow for two actuation modes. However, this is outside the scope of this paper. Introducing the actuation vector at the junction, and stating continuity of deflection and slope and equilibrium of moments and forces, yields

$$\begin{bmatrix} 1 & 1 \\ -\mathrm{j} & -1 \end{bmatrix}\boldsymbol{\Psi}_{\mathbf{a}^+}\mathbf{a}^+ + \begin{bmatrix} 1 & 1 \\ \mathrm{j} & 1 \end{bmatrix}\boldsymbol{\Psi}_{\mathbf{a}^-}\mathbf{a}^- = \begin{bmatrix} 1 & 1 \\ -\mathrm{j}\gamma & -\gamma \end{bmatrix}\boldsymbol{\Psi}_{\mathbf{b}^+}\mathbf{b}^+, \tag{17a}$$

$$\begin{bmatrix} 1 & -1 \\ \mathrm{j} & -1 \end{bmatrix}\boldsymbol{\Psi}_{\mathbf{a}^+}\mathbf{a}^+ + \begin{bmatrix} 1 & -1 \\ -\mathrm{j} & 1 \end{bmatrix}\boldsymbol{\Psi}_{\mathbf{a}^-}\mathbf{a}^- = \alpha\begin{bmatrix} 1 & -1 \\ \mathrm{j}\gamma & -\gamma \end{bmatrix}\boldsymbol{\Psi}_{\mathbf{b}^+}\mathbf{b}^+ - \mathbf{Q}^{\mathrm{act}}. \tag{17b}$$

Substituting Eqs. (8a,b) and (16) into Eqs. (17a) and (17b) gives the transmission and reflection matrices. They will include a term containing the introduced external force, F^{act}. Further, as the incoming near field is neglected, the transmission and reflection matrices will contain non-zero elements only in their first columns. These, in total four, elements will be referred to as the active scattering factors, two for reflection and two or

transmission. Performing the calculations yield

$$r_p^{\text{act}} = r_p^{\text{pass}} + \frac{F^{\text{act}}}{2k_1^3 EI_1 a_p^+} \quad \frac{-\gamma(1+\text{j}) + \alpha\gamma(1-\text{j}) - 2\text{j}\alpha}{\Delta}, \tag{18a}$$

$$r_N^{\text{act}} = r_N^{\text{pass}} + \frac{F^{\text{act}}}{2k_1^3 EI_1 a_p^+} \quad \frac{(\text{j}-1)(\alpha(1+\gamma) + \text{j}(\alpha+\gamma))}{\Delta}, \tag{18b}$$

$$t_p^{\text{act}} = t_p^{\text{pass}} + \frac{F^{\text{act}}}{2k_1^3 EI_1 a_p^+} \quad \frac{-\alpha(1+\text{j}) + (1-\text{j}) - 2\text{j}\gamma}{\Delta}, \tag{18c}$$

$$t_N^{\text{act}} = t_N^{\text{pass}} + \frac{F^{\text{act}}}{2k_1^3 EI_1 a_p^+} \quad \frac{\alpha(\text{j}-1) + (1+\text{j}) + 2\text{j}\gamma}{\Delta}, \tag{18d}$$

where p and N again denote propagating wave and near field, respectively, and the terms superscripted by *pass* are the equivalent terms found in the respective matrices in Eqs. (13a) and (13b). Again the connection point has been chosen at $x = 0$.

3.2. Control laws based on manipulation of the scattering properties

Implementing active control of the bending waves at the junction between the two beams means using the external force F^{act} to influence the amplitudes of the scattered field or the scattering factors themselves. Thus control laws can be derived from Eqs. (18a–d) by putting constraints on the scattering factors. With respect to these scattering factors, two control laws are obvious: suppressing reflection ($r_p^{\text{act}} = 0$) or transmission ($t_p^{\text{act}} = 0$) of the incoming wave field. To derive the control force for a non-reflective junction, the left side in Eq. (18a) is set to zero and the active force is calculated to give

$$F_{\text{no ref}}^{\text{act}} = k_1^3 EI_1 a_p^+ \frac{(1+\text{j})(-2\alpha(1-\gamma^2)) + \text{j}\gamma(1-\alpha)^2}{\gamma(\alpha-\text{j}) + \alpha(1-\text{j})}. \tag{19}$$

In analogy, the control force for the case of a non-transmissive junction can be derived by setting the left side of Eq. (18c) to zero and solving for the active force:

$$F_{\text{no trans}}^{\text{act}} = 4k_1^3 EI_1 a_p^+ \text{j} \frac{(1+\alpha)(1+\gamma)}{\alpha(1+\text{j}) + (\text{j}-1) + 2\text{j}\gamma}. \tag{20}$$

Results of how these control laws depend on their parameters α and γ will be presented in Section 5. These control laws require information about the properties of the connected beams and have a linear dependence on the amplitude of the incoming wave, a_p^+.

4. Junction power flow

4.1. Active power scattering properties

So far only vibration amplitudes have been considered, but to get a complete view of how the junction behaves it is important to investigate the power flow. This is also important when specifying control objectives. The power associated with each propagating wave (i.e. no near fields are considered) is independently calculated as

$$W_p = \tfrac{1}{2}\text{Re}\{F\dot{w}^*\} + \tfrac{1}{2}\text{Re}\{M\dot{\beta}^*\}, \tag{21}$$

where the dot and $*$ indicate time derivative and complex conjugate, respectively, and Re denotes that the real part of the argument is extracted. Here it can be noted that one near field by itself does not propagate power, and this is why they could be neglected in this case. However, the combination of two opposite near fields may propagate power and must in that case be taken into account.

Waves propagating in the positive direction are defined as carrying positive power and negatively propagating waves are defined to carry negative power. Three power waves can be calculated, two on the left side of the junction and one on the right side. In order to fulfil the condition of power conservation, the sum of the power flow on the left side has to be equal to the sum of the power flow on the right side and the power introduced or removed by the active force. Using Eq. (21) the power associated with each propagating wave can be calculated:

$$W_1^+ = EI_1 k_1^3 |a_p^+|^2, \tag{22a}$$

$$W_1^- = EI_1 k_1^3 |a_p^+|^2 |r_p^{\text{act}}|^2, \tag{22b}$$

$$W_2^+ = EI_2 k_2^3 |a_p^+|^2 |t_p^{\text{act}}|^2. \tag{22c}$$

The elements in the scattering vector that affect the transmitted and reflected waves have been substituted into Eqs. (22a–c) in order to express the propagating power in terms of the active scattering factors. The active force power input can be calculated as

$$W_{\text{in}} = \tfrac{1}{2}\text{Re}\{F^{\text{act}}\dot{w}^*\}. \tag{23}$$

A transmission efficiency for the active junction can be defined as the ratio of positive power transport on each side of the discontinuity according to

$$\tau = \frac{W_2^+(x=0)}{W_1^+(x=0)}. \tag{24}$$

Similarly a reflection efficiency can be defined as the ratio of the reflected power to the incoming power like

$$R = \frac{W_1^-(x=0)}{W_1^+(x=0)}. \tag{25}$$

Note that the term 'efficiency' (transmission and reflection) here is used to describe power ratios, while the term 'factor' (transmission and reflection) was previously used to describe amplitude ratios. Substituting Eqs. (22c) and (22a) into Eq. (24) gives the active transmission efficiency as

$$\tau^{\text{act}} = \text{Re}\{\alpha\gamma\}|t_p^{\text{act}}|^2. \tag{26}$$

Similarly, by substituting Eqs. (22b) and (22a) into Eq. (25), the reflection efficiency may be expressed as

$$R^{\text{act}} = |r_p^{\text{act}}|^2. \tag{27}$$

This is well-established knowledge [1] for power transmission and reflection for the passive case. However, it may here be important to point out that these indices are calculated with the active force working in the system. Hence, although the dependence of the active transmission and reflection efficiencies R^{act} and τ^{act} is similar for the active and the passive case, their values may differ because of their implicit active force dependence. One can also see that for a given control law, τ^{act} and R^{act} are entirely dependent on the factors α and γ. This becomes apparent if we substitute one of the active force expressions, Eqs. (19) or (20), into either of Eqs. (18a) or (18c) in which the terms $a_p^+ k_1^3 EI_1$ cancel out each other.

From this two interesting conclusions can be drawn: firstly, since the factors α and γ are fractions of wavenumbers and bending stiffnesses, the transmission and reflection efficiencies for a given control law are frequency independent; and secondly, there are four physical beam properties that will influence the power transmission and reflection, namely Young's modulus, density, and cross-sectional height and width.

4.2. Control law based on power considerations

The control laws derived in the previous section were based on forcing the active scattering factors to zero, which gave simple calculations for the active force. The control objectives might also be based on power considerations. A straightforward situation would be that it is desirable to minimise the power flowing from the junction back into the beams. Thus the sum of the reflected and transmitted power

ought to be minimised. As an appropriate index, the sum of the reflection and transmission efficiencies can be defined:

$$S^{\mathrm{act}} = R^{\mathrm{act}} + \tau^{\mathrm{act}}. \tag{28}$$

Since in the passive case S would always be equal to one, the active force has to account for its discrepancy from one. Thus minimising S^{act} is equivalent to maximising the power absorbed by the active force (W_{in}). In order to minimise the quantity, S^{act}, its derivative is set to zero, according to

$$\frac{\partial S^{\mathrm{act}}}{\partial F^{\mathrm{act}}} = 0, \tag{29}$$

where the derivative is taken with respect to the real and imaginary parts of the active force separately. If the expressions for active transmission and reflection factors, Eqs. (18a) and (18c), are substituted into the transmission and reflection efficiencies (Eqs. (26) and (27)) and inserted into Eq. (28), the minimisation problem reduces to the well-known minimisation of quadratic forms for complex-valued functions; see e.g. Ref. [17]. Thus Eq. (28) can be written in the form,

$$S^{\mathrm{act}} = |F^{\mathrm{act}}|^2 A + F^{\mathrm{act}} b^* + F^{\mathrm{act}*} b + c, \tag{30}$$

where c, b and A are recognised as

$$c = \alpha\gamma |t_p^{\mathrm{pass}}|^2 + |r_p^{\mathrm{pass}}|^2, \tag{31a}$$

$$b = \alpha\gamma t_p^{\mathrm{pass}} \sigma_t^* + r_p^{\mathrm{pass}} \sigma_r^*, \tag{31b}$$

$$A = \alpha\gamma |\sigma_t|^2 + |\sigma_r|^2 \tag{31c}$$

and σ_r and σ_t are given by

$$\sigma_r = \frac{-\gamma(1+\mathrm{j}) + \alpha\gamma(1-\mathrm{j}) - 2\mathrm{j}\alpha}{2k_1^3 EI_1 a_p^+ \Delta}, \tag{32a}$$

$$\sigma_t = \frac{-\alpha(1+\mathrm{j}) + (1-\mathrm{j}) - 2\mathrm{j}\gamma}{2k_1^3 EI_1 a_p^+ \Delta}, \tag{32b}$$

respectively. The indices σ_r and σ_t are results from factoring what is to the right of the plus sign in Eqs. (18a) and (18c), into F^{act} times a scaling factor. Eq. (30) has a unique minimum at

$$\frac{\partial S^{\mathrm{act}}}{\partial F^{\mathrm{act}}} = 0 \Rightarrow \min(S^{\mathrm{act}}) = c - \frac{|b|^2}{A}, \tag{33}$$

which appears for the active force

$$F_0^{\mathrm{act}} = -\frac{b}{A}. \tag{34}$$

These are then referred to as the optimal active force and scattering efficiency for this case. If Eqs. (31b) and (31c) are inserted into Eq. (34), the control law takes a form more similar to the other control laws derived:

$$F_{\mathrm{opt}}^{\mathrm{act}} = -k_1^3 EI_1 a_p^+ \frac{\gamma(1+\mathrm{j}) + \alpha\gamma(\mathrm{j}-1) + 2\mathrm{j}\alpha}{\alpha+\gamma}. \tag{35}$$

5. Results

Several figures are presented in this section. The transmission efficiency for the control law of a non-reflective junction is plotted against the parameters α and γ in Fig. 3. A bold line in the figure denotes where the transmission efficiency is equal to one (zero dB). The reflection efficiency for the non-transmissive junction is not depicted, as it is equal to one for all parameter combinations. This is accounted for

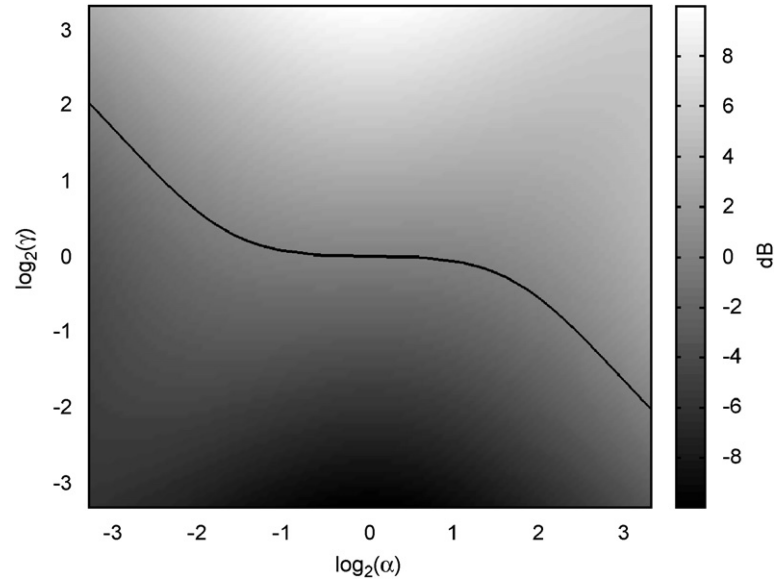

Fig. 3. Transmission efficiency ($\tau^{\text{act}}_{\text{no ref}}$) as a function of the parameters α and γ, for the control law of a non-reflective junction. The section where $10\log_{10}(\tau^{\text{act}}_{\text{no ref}}) = 0$ is highlighted.

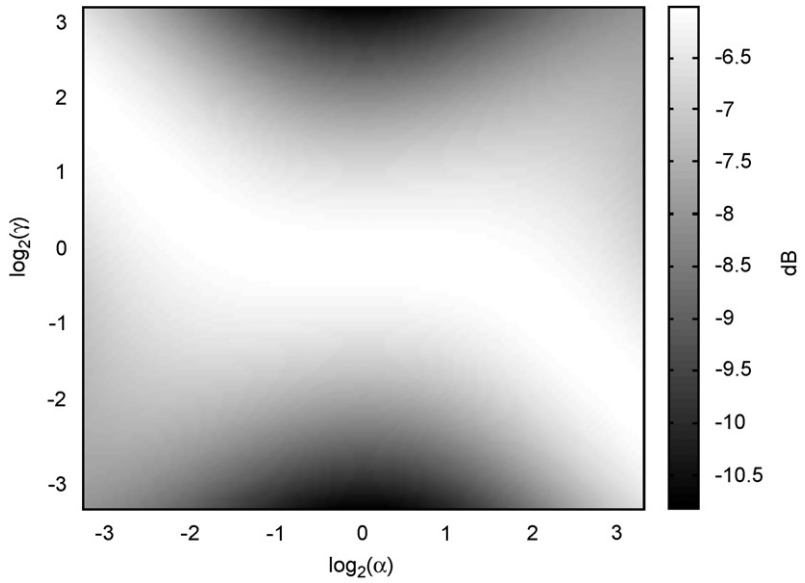

Fig. 4. Transmission efficiency ($\tau^{\text{act}}_{\text{opt}}$) as a function of the parameters α and γ, for the control law of maximum power absorption.

by the purely imaginary input mobility, at the active force location, when only a near field is present in the right-side beam.

The transmission and reflection efficiencies for the control law of optimal power absorption are depicted in Figs. 4 and 5. Their sum, S^{act}, is depicted in Fig. 6. The magnitudes of the control forces as functions of the parameters α and γ are plotted for the three different control laws, Figs. 7–9. They are normalised with $k_1^3 EI_1 a_p^+$ in order to make the control forces solely dependent on α and γ. All results are presented in a dB scale. The function axis are presented with a logarithmic scale using the base two, because it represents a doubling of the variable.

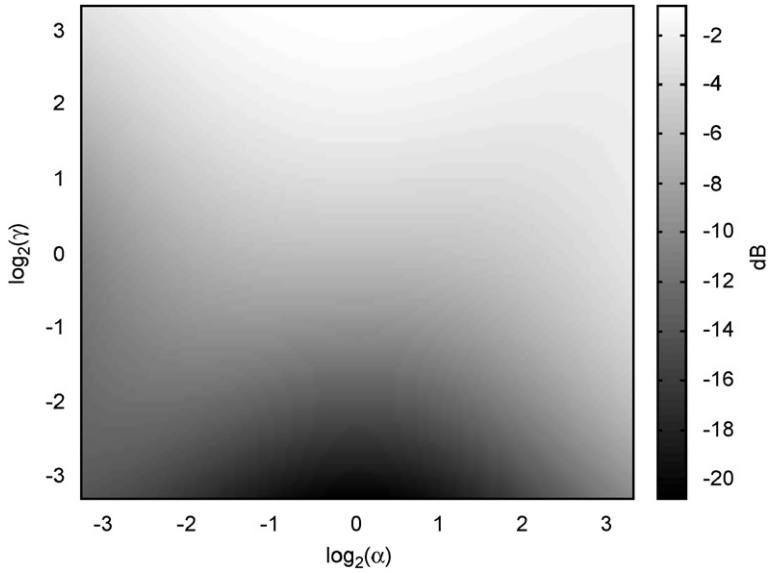

Fig. 5. Reflection efficiency ($R_{\text{opt}}^{\text{act}}$) as a function of the parameters α and γ, for the control law of maximum power absorption.

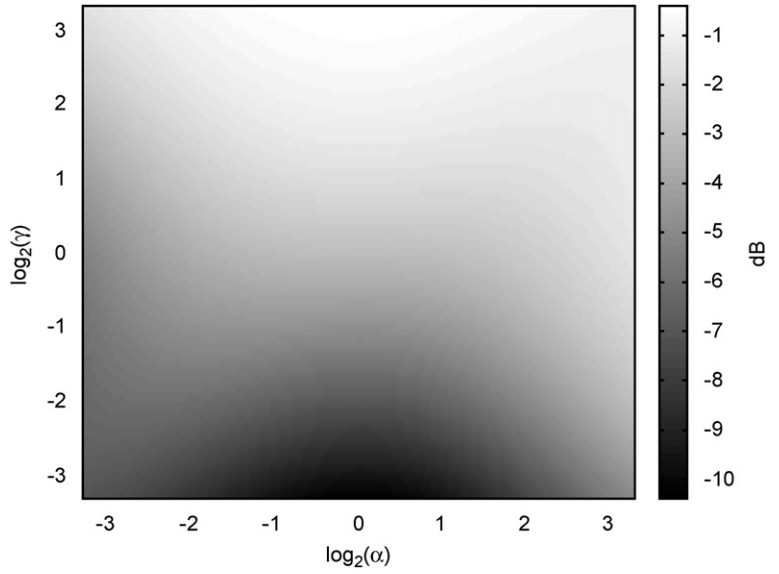

Fig. 6. Total scattered power ($S_{\text{opt}}^{\text{act}}$) as a function of the parameters α and γ, for the control law of maximum power absorption.

6. Discussion

6.1. Ideal termination cases

To facilitate any interpretation of the results given in Figs. 3–9 it may be helpful to illustrate how the change of the physical beam parameters influence the values of the dimensionless parameters α and γ. For beams with rectangular cross sections, expressions of the parameters α and γ as explicit functions of the physical beam geometry and material properties can be obtained by substituting the relation

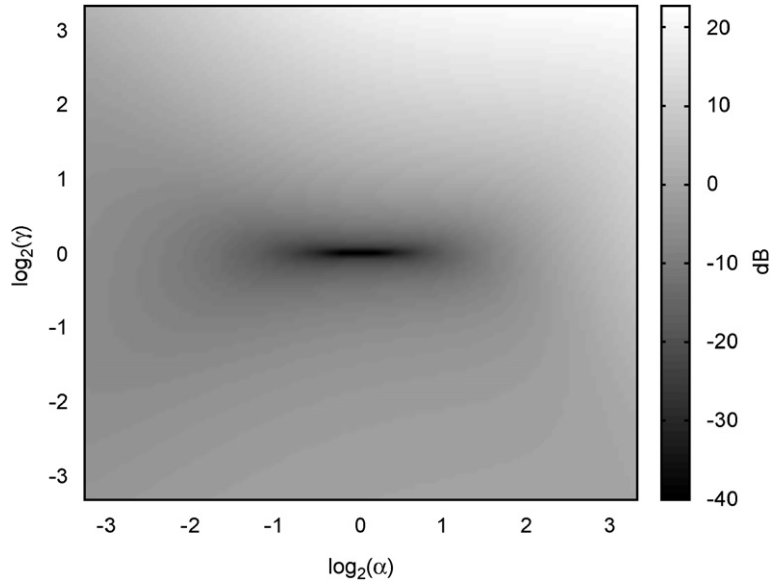

Fig. 7. The active force magnitude, for the control law of a non-reflective junction, as a function of the parameters α and γ, normalised with $k_1^3 EI_1 a_p^+$.

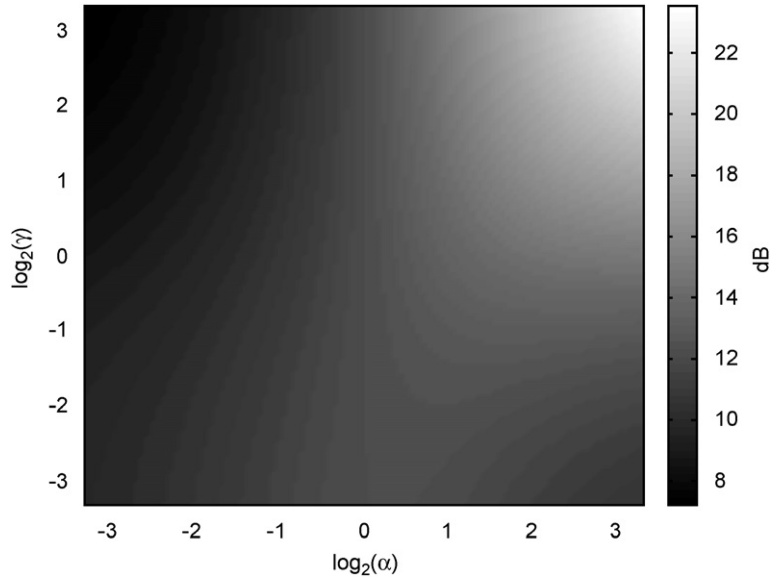

Fig. 8. The active force magnitude, for the control law of a non-transmissive junction, as a function of the parameters α and γ, normalised with $k_1^3 EI_1 a_p^+$.

for the bending wavenumber of Eq. (5) into Eqs. (12a,b) together with the relations for rectangular cross sections:

$$S = bh, \quad I = \frac{bh^3}{12}, \tag{36a,b}$$

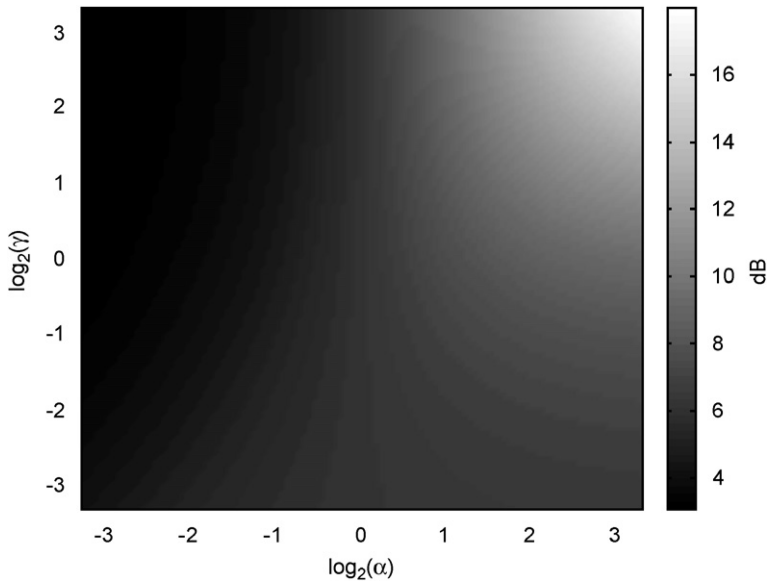

Fig. 9. The active force magnitude, for the control law of maximum power absorption, as a function of the parameters α and γ, normalised with $k_1^3 EI_1 a_p^+$.

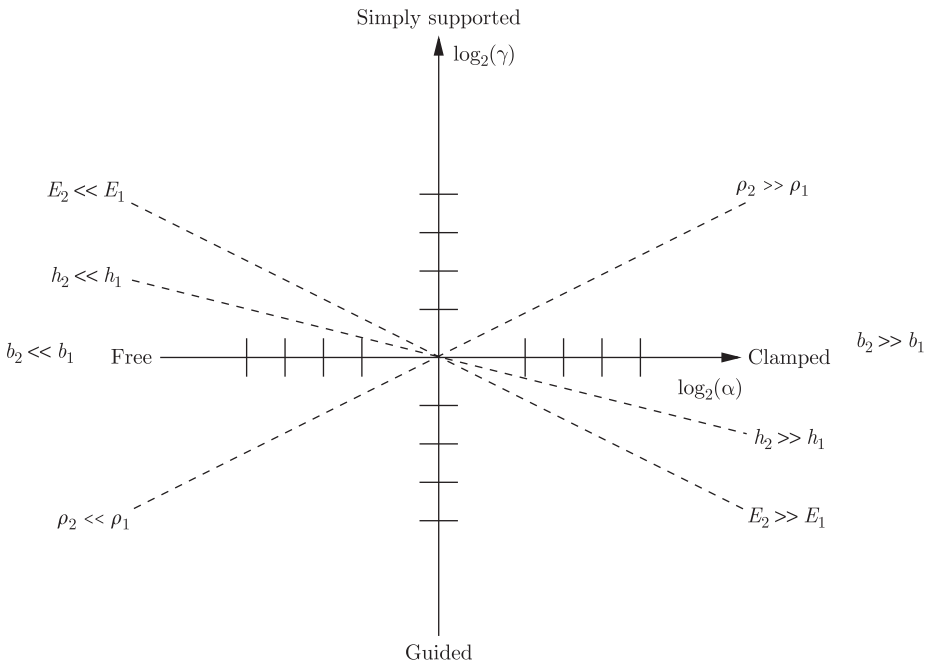

Fig. 10. This figure depicts in which directions the ideal termination cases are found. It also shows the rate at which the parameters $\log_2(\alpha)$ and $\log_2(\gamma)$ change when changing the ratio between any of the physical beam properties.

where S is the cross-sectional area and I the inertia. This gives

$$\alpha = \frac{b_2 h_2^2}{b_1 h_1^2} \sqrt{\frac{\rho_2 E_2}{\rho_1 E_1}}, \tag{37a}$$

$$\gamma = \sqrt[4]{\frac{\rho_2 h_1^2 E_1}{\rho_1 h_2^2 E_2}}, \tag{37b}$$

where h and b are the cross-sectional dimensions height and width, respectively. E is the Young's modulus and ρ is the density.

Eqs. (37a) and (37b) show that the cross-sectional height and the Young's modulus have a similar impact in changing the parameters α and γ. However, the rate of the change, which is given by respective exponent, is quite different. Comparable conclusions may be drawn for any other physical beam parameter: they all appear as ratios with different exponents. This directly leads to Fig. 10, where the dependency of α and γ from changes in the ratio of all physical beam parameters are given in the $\log_2(\alpha) - \log_2(\gamma)$ plane.

Changing the ratio of one of these physical parameters means moving along straight lines with different slopes. Changing the Young's modulus ratio is equivalent to moving along a line with the slope -0.5 from the upper left corner ($E_2 \ll E_1$) to the lower right corner ($E_2 \gg E_1$). Changing the cross-sectional height mean moving along the same diagonal but with the slope -0.25. Changing the density ratio is equivalent to moving along a diagonal line (with slope 0.5) from the lower left corner ($\rho_2 \ll \rho_1$) to the upper right corner ($\rho_2 \gg \rho_1$) in the $\log_2(\alpha) - \log_2(\gamma)$ plane. Changing the cross-sectional width means moving along a horizontal line at $\gamma = 0$.

It can be seen from Eqs. (37a) and (37b) that the specific straight lines in Fig. 10 are obtained if the remaining physical beam parameters ratios are one. For other ratios of the remaining physical beam parameters the dashed lines must be shifted in parallel. Thus in order to move away from any of the dashed lines in Fig. 10, two or more of the physical beam parameters must be different.

These equations also help to simplify where the four ideal termination cases appear. Suppose that the rates of change of the density and the Young's modulus are equal. The free end case would mean a negligible density and bending stiffness in the right-side beam compared to the left-side beam, and thus $\log_2(\alpha) \to -\infty$ and $\log_2(\gamma) = 0$. To approach the clamped case means moving in the opposite direction, $\log_2(\alpha) \to \infty$ and $\log_2(\gamma) = 0$. For the simply supported case, the density of the right-side beam becomes large while the bending stiffness becomes low, $\log_2(\alpha) = 0$ and $\log_2(\gamma) \to \infty$. Moving in the opposite direction of that means approaching the guided termination case; see Fig. 10.

Making any one of the physical parameters in the right-side beam much larger compared to the left-side beam means moving towards the clamped case, as the rate of change is much larger for α than for γ. Analogously, making any of the physical beam parameters in the right-side beam negligible compared to the left-side beam implies moving towards the free end case.

6.2. Non-reflective junction

Fig. 3 shows an interesting aspect. The transmission efficiency is equal to one (zero dB) for certain non-trivial combinations of α and γ situated along a curved line as indicated in Fig. 3. Thus the active force inserts no power. Hence there are ratios of wavenumbers and bending stiffnesses which give a conservative junction while still fulfilling the control criterion of a non-reflective junction. This implies that there is a certain value of α and γ for which a reactive (passive) system is enough in order to achieve a non-reflective junction. For which parameter values $\tau^{\text{act}} = 1$ can be calculated by setting Eq. (26) equal to one and then expressing one of the parameters as a function of the other one.

There is another interesting observation to be made when studying Fig. 3. Given a choice, there are some α and γ relations which are advantageous in terms of power absorption. If one beam is connected to another beam of known material parameters and cross-sectional dimensions, it is possible to choose the second beam in a way that ensures the junction to be absorptive, in the region below the bold line in Fig. 3. Thus for the control law of a non-reflective junction the active force removes power from the system. This provides very interesting information when choosing a control law for a real-life implementation. Choosing this control objective, it is possible to specify the physical parameters of the right-side beam in such a way that the active force and right-side beam configuration always draw power out of the left-side beam. This controller might in many cases be advantageous to a pure optimal absorption controller, which almost certainly will reflect a

certain amount of the incident power. Compare with Fig. 5 which only approaches zero reflected power when moving towards the ideal termination cases, free end and guided.

The force required to create a non-reflective junction (Fig. 7) reaches a minimum around the area where α and γ are close to unity. This seems very reasonable, as no force is required in order to create a non-reflective junction between two identical beams, which simply corresponds to one continuous beam. Away from this area, though, the force magnitude does not grow symmetrically. For the case where α and γ are large, the force required is much bigger than for the opposite case. This might be explained by the increasingly large near field when going from a beam with a low value for k and EI to a beam with a higher value. This is a result of having a prescribed wave amplitude in the left-side beam. Identical wave amplitudes but different k and EI result in different power carried by the incident wave. The non-symmetry phenomenon can be seen in the figures of the force magnitude for the non-transmissive junction (Fig. 8) and for the optimal force (Fig. 9).

The force magnitude, Fig. 7, reaches a maximum when approaching the corner between the simply supported and the clamped termination. This ought to be a result of the weak coupling between the actuation mode (force) and the degree of freedom to be influenced (rotation) at the simply supported termination, and the inability to influence any of the degrees of freedom at a clamped termination. Similar phenomena are also visible in Figs. 8 and 9.

In order to achieve a non-reflective junction for the simply supported termination case, a moment actuation would be preferable. In general it seems that the non-reflective junction requires a lower control force compared to the two others. Overall the control forces increase as α and γ increase, since it then becomes harder to move the right-side beam.

6.3. Non-transmissive junction

The force magnitude for the non-transmissive junction, Fig. 8, is the control law which requires the largest control effort of the three investigated ones. It goes towards a minimum when α becomes small and γ becomes large and towards a maximum when both parameters increase. Fig. 8 suggests that, when approaching the ideal termination cases where the deflection degree of freedom is locked (i.e. clamped and simply supported termination), the force magnitude increases. This is despite the small deflection that needs to be corrected for. Even for a small deflection amplitude, a great force is required when the parameters α and γ are large.

6.4. Optimal junction

For the homogeneous beam case ($\alpha = \gamma = 1$) the best that can be achieved by an optimal absorbing control force is that half of the incident power is absorbed by the active force, while the other half is scattered. This can be seen in Fig. 6 at the point where $\log_2(\alpha) = \log_2(\gamma) = 0$, where $S^{\text{act}} = -3\,\text{dB}$. Further, Figs. 4 and 5 show that for this case one quarter ($-6\,\text{dB}$) of the incident power is reflected while one quarter is transmitted. This is a result previously reported by Guicking [15].

When approaching the free end case, the total scattered power reduces; see Fig. 6. In theory all power can be actively absorbed at a free end. This has also been experimentally verified by Scheuren [9]. However, a minimum is reached faster when moving towards the guided termination. Moving in the opposite direction of the guided termination towards the simply supported case, almost no power absorption is possible. This ought to be a result of the weak coupling between the actuation mode (force) and the degree of freedom to be influenced (rotation). Further, a large γ means that the bending wave number for the right-side beam is much larger than that for the left-side beam. As in the equation for the power carried by a wave (Eq. (22c)), the wavenumber is cubed; even a small wave amplitude in the right-hand side beam would mean a substantial amount of power. Thus the optimal control force aims at transmitting almost no power and, as almost no power can be absorbed, most of the power is instead reflected (see Figs. 4 and 5).

7. Conclusions

The formalism of the derivations, together with expressing the active scattering factors in a force term and a passive term, is helpful for a physical understanding. It distinguishes the mechanism of the active force in a

clear way. It enables the derivation of control laws by simple manipulation of the active scattering vector. These control laws can, after normalisation, be expressed in a two-dimensional space (plane). In their limits these planes contain the ideal beam termination cases such as a free end, clamped end, simply supported and guided termination. The results agree with previously presented results regarding active control at a beam boundary.

Results show that for the case of the non-reflective junction the right-side beam can be chosen in such a way that the active force and beam configuration always draw power from the left-side beam. To experimentally verify these results together with considering dissipative elements are natural extensions of the work presented here.

Acknowledgements

This work is funded by the Swedish research council, project: 621-2004-5185.

References

[1] L. Cremer, M. Heckl, B. Petersson, *Structure-Borne Sound*, Springer, Berlin, 2005.
[2] B. Mace, Wave reflection and transmission in beams, *Journal of Sound and Vibration* 97 (1984) 237–246.
[3] C. Mei, B. Mace, Wave reflection and transmission in Timoshenko beams and wave analysis of Timoshenko beam structures, *Transcations of the American Society of Mechanical Engineering* 127 (2005) 382–394.
[4] D. Miller, Modelling and Active Modification of Wave Scattering in Structural Networks, PhD Thesis, Massachussets Institute of Technology (1988).
[5] D. Miller, A. von Flotow, A travelling wave approach to power flow in structural junctions, *Journal of Sound and Vibration* 128 (1989) 145–162.
[6] D. Miller, S. Hall, A. von Flotow, Optimal control of power flow at structural junctions, *Journal of Sound and Vibration* 140 (1990) 475–497.
[7] D. Miller, A. von Flotow, S. Hall, Active modification of wave reflection and transmission in flexible structures, *Proceedings of the 1987 American Control Conference*, Vol. 2, 1987, pp. 1318–1324.
[8] A. von Flotow, B. Schäfer, Wave-absorbing controllers for a flexible beam, *Journal of Guidance* 9 (1986) 673–680.
[9] J. Scheuren, Non-reflecting termination for bending waves in beams by active means, *Proceedings of the 1988 International Conference on Noise Control Engineering*, Noise Control Foundation, 1988, pp. 1065–1068.
[10] R. Gonzalez, F. Bustamente, Active control of the reflection of waves in beams, *Proceedings of the SPIE—The International Society for Optical Engineering*, Vol. 4326, 2001, pp. 77–88.
[11] J. Hu, J.-F. Lin, Active impedance control of linear one-dimensional wave equations, *International Journal of Control* 72 (1999) 247–257.
[12] R. McKinnel, Active vibration isolation by cancelling bending waves, *Proceeding of the Royal Society of London* 421 (1989) 357–393.
[13] B. Mace, Active control of flexural vibrations, *Journal of Sound and Vibration* 114 (1987) 253–270.
[14] J. Scheuren, Active attenuation of bending waves in beams, *Proceedings of the Spring Conference of the Institute of Acoustics in Southampton*, Vol. 12, 1990, pp. 623–629.
[15] D. Guicking, J. Melcher, R. Wimmel, Active impedance control in mechanical structures, *Acustica* 69 (1989) 39–52.
[16] M. Brennan, S. Elliot, R. Pinnington, Strategies for the active control of flexural vibration on a beam, *Journal of Sound and Vibration* 186 (1995) 657–688.
[17] P. Nelson, S. Elliot, *Active Control of Sound*, Academic Press Limited, New York, 1992.